Optica Applicata, Vol. XLII, No. 1, 2012
DOI: 10.5277/oa120101

Multispectral polarized BRDF: design of a highly resolved reflectometer and development of a data inversion method

NICOLAS RIVIERE*, ROMAIN CEOLATO, LAURENT HESPEL

Onera – The French Aerospace Lab, F-31055, Toulouse, France

*Corresponding author: nicolas.riviere@onera.fr

Multispectral and polarized light reflectance measurements are very useful to characterize materials such as paint coatings. This article presents an overview of an automated high-angular resolved, in-plane multispectral polarized reflectometer and its calibration process. A comprehensive study based on multispectral BRDF and DOLP measurements is conducted on different colour and glossy aspects of paint coatings. An original inverse method from in-plane measurements is used to model the out-of-plane BRDF and to investigate the role of the surface and subsurface scattering phenomena in its components.

Keywords: bidirectional reflectance distribution function (BRDF), degree of linear polarization (DOLP), multispectral, polarization, light scattering, paint coatings, inverse method, optimization.

1. Introduction

Optical characterization of materials is particularly needed in different activities ranging from aerospace or automobile industry (quality control, roughness measurements, *etc*.) to remote-sensing (instrument calibration, target reflectance, *etc*.) including defence or security applications (laser imaging, guidance, *etc*.) Bidirectional reflectance of materials is a useful way to probe physical properties of materials. Most of them are considered as ideal Lambertian reflectors that scatter light uniformly in space. However, this approximation does not stand for man-made materials (ceramics, composites, plastic compounds or paint coatings). They require accurate measurements of the bidirectional reflectance distribution function (BRDF) to quantify how light is angularly and spectrally reflected by a material surface. From polarized BRDF, one can also determine degree of linear polarization (DOLP) to quantify and inspect how surface reflection affect light polarization states. Both BRDF and DOLP give a good insight and a better understanding of the scattering processes involved.

Different instruments are designed to measure the BRDF of samples. Some are dedicated only to measure the light backscattered by the media [1–4]. Others are used to estimate the light reflected and/or transmitted [5, 6]. A few of them are to measure

polarized BRDF at fixed wavelength, and they often take into account an angular resolution of the BRDF ranging from 2° to 10° [7–9].

The purpose of this paper is to report the calibration process of a fast and highly resolved instrument dedicated to measure the in-plane multispectral polarized BRDF and DOLP. An original multispectral method based on the inversion of experimental in-plane BRDF data was developed to retrieve the full BRDF. Then, we present BRDF and DOLP measurements on paint coatings to illustrate the capacity of our instrument and our inversion method. Using this approach, we separate the different scattering processes involved from multispectral and polarized measurements and can retrieve the full BRDF from in-plane BRDF measurements.

2. Theoretical framework

2.1. Bidirectional reflectance distribution function (BRDF)

Materials reflect light in a certain way according to the incident light direction and viewing angles. A comprehensive way to characterize the reflectance properties of the scattering media is to evaluate its full BRDF. It fully characterizes the local light scattering by the material for every set of angles. Figure 1 shows the geometry used to define the full BRDF in a three-dimensional standard Cartesian coordinate system.

The BRDF is a non-integrated parameter defined by NICODEMUS [10] as:

$$\mathrm{BRDF}(\theta_i, \phi_i; \theta_r, \phi_r; \lambda) = \frac{\mathrm{d}L_r(\theta_i, \phi_i; \theta_r, \phi_r; \lambda)}{\mathrm{d}E_i(\theta_i, \phi_i; \lambda)} \quad [\mathrm{sr}^{-1}] \tag{1}$$

where, for a particular wavelength: $\mathrm{d}L_r(\theta_i, \phi_i; \theta_r, \phi_r; \lambda)$ is the differential reflected radiance in the direction $\Omega_r = (\theta_r, \phi_r)$; $\mathrm{d}E_i(\theta_i, \phi_i; \lambda)$ is the differential incident irradiance from direction $\Omega_i = (\theta_i, \phi_i)$.

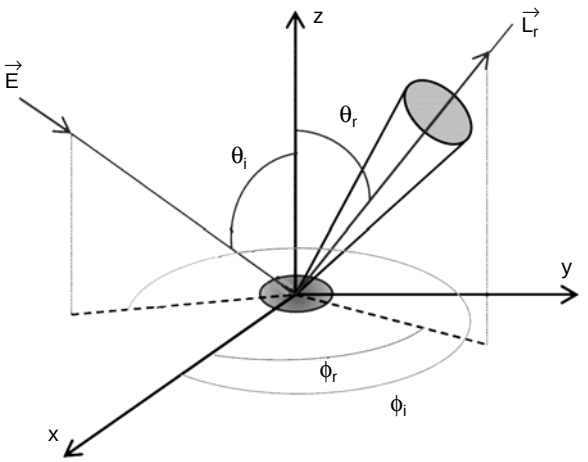

Fig. 1. Definition of the BRDF in a three-dimensional Cartesian coordinate system.

We distinguish the in-plane BRDF as BRDF(θ_i, ϕ_i; θ_r, $\phi_r = \phi_i$; λ) from the out-of--plane BRDF defined as BRDF(θ_i, ϕ_i; θ_r, $\phi_r \neq \phi_i$; λ). The Lambert law induces a cosine factor in radiance measurements. For this reason, we choose to use BRDF$\cos(\theta_i, \phi_i; \theta_r, \phi_r; \lambda)$ = BRDF(θ_i, ϕ_i; θ_r, ϕ_r; λ)$\cos(\theta_r)$.

2.2. Directional hemispheric reflectance (DHR)

Directional hemispheric reflectance (DHR) is an integrated parameter calculated as a ratio of the total reflected energy to the total incident energy from a given direction. Also, it can be computed by integrating the BRDF over the half-space [11] as:

$$\mathrm{DHR}(\theta_i, \phi_i; \lambda) = \int_0^{2\pi} \int_0^{\pi/2} \mathrm{BRDF}(\theta_i, \phi_i; \theta_r, \phi_r; \lambda) \cos(\theta_r) \sin(\theta_r)\, \mathrm{d}\theta_r\, \mathrm{d}\phi_r \tag{2}$$

2.3. Degree of linear polarization

BRDF definition can be extended to a polarized-BRDF^{k,j} to determine DOLP from cross-polarized BRDF^{k,j}:

$$\mathrm{BRDF}^{k,j}(\theta_i, \phi_i; \theta_r, \phi_r; \lambda) = \frac{L_r^{k,j}(\theta_i, \phi_i; \theta_r, \phi_r; \lambda)}{E_i^{k}(\theta_i, \phi_i; \lambda)} \tag{3}$$

$$\mathrm{DOLP}(\theta_i, \phi_i; \theta_r, \phi_r; \lambda) = \frac{\mathrm{BRDF}^{P,P}(\theta_i, \phi_i; \theta_r, \phi_r; \lambda) - \mathrm{BRDF}^{P,S}(\theta_i, \phi_i; \theta_r, \phi_r; \lambda)}{\mathrm{BRDF}^{P,U}(\theta_i, \phi_i; \theta_r, \phi_r; \lambda)} \tag{4}$$

where: $L_r^{k,j}$ is the measured radiance with *k*, *j* referring to the polarization states (*P*: parallel, *S*: perpendicular, *U*: unpolarized) of the incident and detected light, respectively.

3. Numerical model and data inversion

The BRDF of materials can be represented by mathematical models. Different BRDF semi-empirical models were developed for various applications: deterministic (fully based on electromagnetism without data) [12, 13], physical (data interpolation using physical parameters) [14–16] and empirical models (data interpolation using non-physical parameters) [17]. In this paper, the Li–Torrance model [16] is adapted to our experimental data for multispectral BRDF inversion.

3.1. Li–Torrance BRDF model

The light scattered from a material can be divided into two parts: surface scattering referring to light scattered at the material surface and subsurface scattering referring

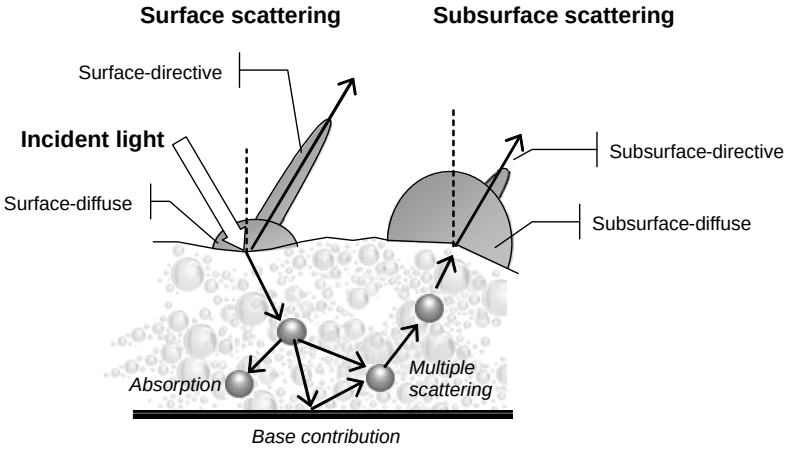

Fig. 2. Light scattering from material: surface and subsurface contributions.

to light scattered within the material (Fig. 2). Both scattering phenomena result from single and multiple scattering. Furthermore, one should consider the complex optical index m of the scattering media as $m = n + i\kappa$, where n and κ are respectively the real and the imaginary parts of the complex optical index. Absorption phenomena result in $\kappa \neq 0$.

On the one hand, surface scattering is composed of:

– a surface directional (or mirror-like) part due to surface reflection. It is related to Fresnel coefficients and to the surface roughness;

– a surface diffuse (or self-shadowing) part due to multiple scattering by the micro-facets.

On the other hand, subsurface scattering is also composed of:

– a subsurface directional part from the base contribution;

– a subsurface diffuse part resulting from multiple scattering inside the material.

Depending on the type of materials, one needs to quantify the contribution of light scattering part in order to apply BRDF model such as Li–Torrance model [18]. In the following, we applied the Li–Torrance model extended to our multispectral measurements to investigate scattering phenomena involved in BRDF. This model incorporates all of the physical phenomena appearing in the He–Torrance model [13] and is described by only 4 k-parameters:

$$\mathrm{BRDF}(\theta_i, \phi_i; \theta_r, \phi_r; \lambda) = \mathrm{BRDF}(k_{dd}, k_{uds}, k_{udf}, k_{fs}) \tag{5}$$

where: k_{dd} is related to the Fresnel coefficients and the roughness of the surface. It contributes to the directional reflection (mirror-like) component and to the first surface directional-diffuse component. k_{uds} accounts for multiple scattering on rough surfaces (Lambertian component) and contributes to the first surface uniform-diffuse compo-

T a b l e 1. Relations between *k*-parameters and BRDF components.

BRDF	Directional component		Diffuse component	
Scattering phenomena	Surface--directional	Subsurface--directional	Surface-diffuse (self-shadowing)	Subsurface uniform-diffuse
	k_{dd}	k_{fs}	k_{udf}	k_{uds}

nent. k_{udf} is related to the directional-hemispherical reflectance of the subsurface and to the Fresnel transmission coefficient. It contributes to the subsurface uniform--diffuse component. k_{fs} is an empirical BRDF model based on functional reasoning and data fitting. It contributes to the subsurface forward-scattering component. These *k*-parameters are related to the BRDF directional and diffuse components (Tab. 1).

We extended the Li–Torrance model to a multispectral model for our inversion technique. For N different wavelengths, the determination of $4\times N$ *k*-parameters is required to model the multispectral BRDF:

$$\mathrm{BRDF}(\theta_i, \phi_i; \theta_r, \phi_r; \lambda_{1\ldots N}) = \mathrm{BRDF}\left(k_{dd}^{1\ldots N}, k_{uds}^{1\ldots N}, k_{udf}^{1\ldots N}, k_{fs}^{1\ldots N}; \lambda_{1\ldots N}\right) \tag{6}$$

Thus, a $4\times N$-matrix K_N is defined from the *k*-parameters as follows:

$$\mathrm{BRDF}(\theta_i, \phi_i; \theta_r, \phi_r; \lambda_{1\ldots N}) = \mathrm{BRDF}(K_N) \tag{7}$$

where

$$K_N = \begin{bmatrix} k_{dd}^1 & \ldots & \ldots & k_{dd}^N \\ k_{uds}^1 & \ldots & \ldots & k_{uds}^N \\ k_{udf}^1 & \ldots & \ldots & k_{udf}^N \\ k_{fs}^1 & \ldots & \ldots & k_{fs}^N \end{bmatrix} \tag{8}$$

3.2. Data inversion method

For many applications [1, 3, 7, 15, 18], collecting the full-BRDF takes a great effort, and as a consequence only the in-plane BRDF is measured. We propose an inversion method to retrieve the multispectral full-BRDF from highly resolved in-plane BRDF measurements. For a numerically stable data inversion algorithm, high angular resolution is needed for BRDF measurements.

The aim of our method is to retrieve the K_N matrix to model the full BRDF. Because an analytical inversion cannot be achieved for solving nonlinear problems, an optimization technique is performed to identify a complete K_N matrix. Our method

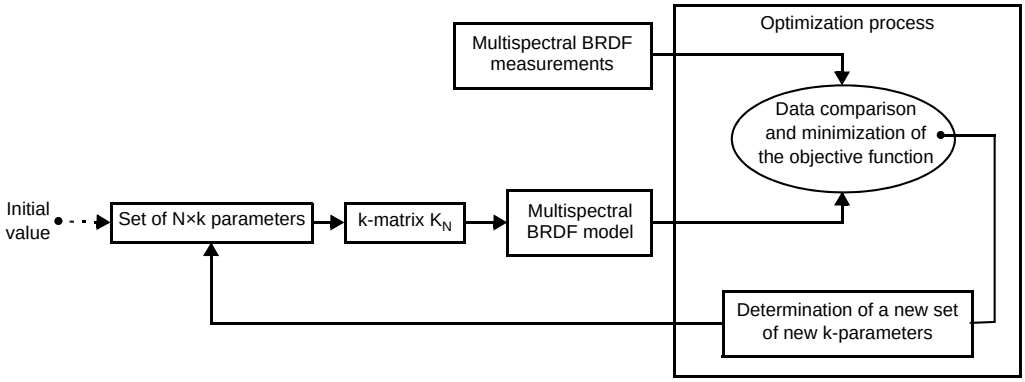

Fig. 3. Data inversion method.

combines a Broyden–Fletcher–Goldfarb–Shanno (BFGS) quasi-Newton optimization technique [19] with the multispectral Li–Torrance BRDF model. Figure 3 describes the optimization schemes.

First, we define an objective function F_j based on various combinations of k-parameters (Li–Torrance model) for a fixed wavelength λ_j:

$$F_j(\Omega_i, \Omega_r; \lambda_j) = \sum_k \left[\frac{\mathrm{BRDF}_{\mathrm{simulated}}^{k_{dd}^j, k_{uds}^j, k_{udf}^j, k_{fs}^j}(\Omega_i, \Omega_r; \lambda_j) - \mathrm{BRDF}_{\mathrm{measurement}}(\Omega_i, \Omega_r; \lambda_j)}{\mathrm{BRDF}_{\mathrm{measurement}}(\Omega_i, \Omega_r; \lambda_j)} \right]^2 \tag{9}$$

where $\Omega_i = (\theta_i, \phi_i)$ and $\Omega_r = (\theta_r, \phi_r)$.

The previous formula is a sum of root mean square differences between measured and simulated in-plane BRDFs. We also define a general objective function F as the sum of objective functions F_j defined for each λ_j (where j ranges from 1 to N) and for each scattered angle:

$$F = \frac{1}{N} \sum_{j=1}^{N} F_j(\Omega_i, \Omega_r; \lambda_j) \tag{10}$$

Then, we minimize F in order to retrieve each k-parameter for each wavelength considered (for an ideal case where the simulated BRDF is equal to the experimental one, F equals zero). From the retrieved K_N matrix, the multispectral full BRDF can be computed. We applied our data inversion method for various coatings as will be shown in Section 5.

4. Reflectometer design and calibration

The BRDF of materials can be measured in experimental setups. An automated and accurate calibration process is needed to measure in-plane multispectral polarized

BRDF and DOLP of different types of samples. Figure 4 shows a general view of our instrument and Fig. 5 describes its optical layout.

The incident lighting system consists of three different laser sources (Nd:Yag laser at 532 nm, He-Ne laser at 633 nm, diode laser at 814 nm) linearly polarized using a wideband polarizer. The detection system measures the in-plane BRDF with an angular resolution lower than 1°. It provides highly resolved reflectance measurements needed for a better data inversion. It is composed of an Si-detector DET-90 (Hinds Instruments) mounted on a rotation stage 1 meter apart from the sample coupled with a wideband polarizer and interferential filters. A simple method based on Fresnel

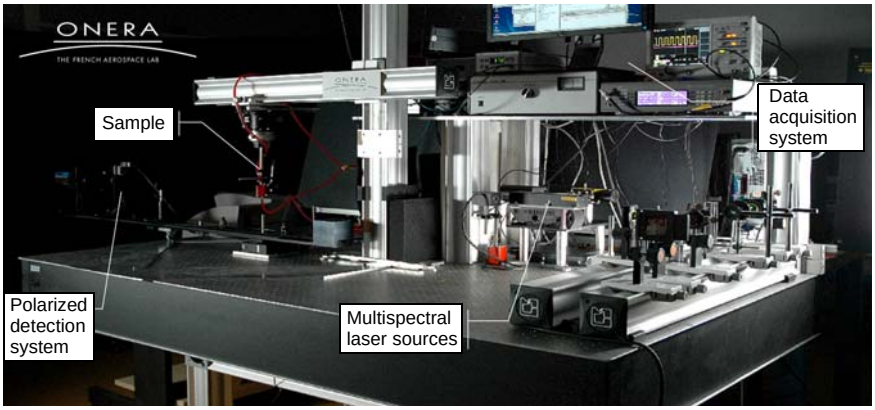

Fig. 4. General view of the instrument.

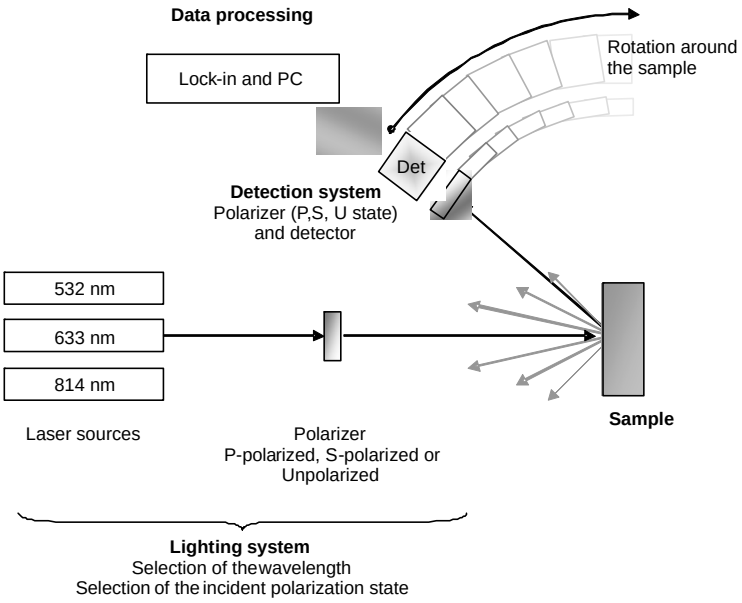

Fig. 5. Optical layout of the instrument.

equations is used to identify polarizer's axes. A lock-in amplifier is used to increase the signal-to-noise ratio for noisy signals. Measurements are fully interfaced via GPIB and PCI cards to control step motors and the lock-in amplifier using homemade software.

For experimental use, we express BRDF with $\Delta\Omega_r = 10^{-4}$ sr the reflected solid angle, $P_i^k(\theta_i, \phi_i; \lambda)$ and $P_i^{k,j}(\theta_i, \phi_i; \theta_r, \phi_r; \lambda)$ the incident and reflected powers, respectively:

$$\mathrm{BRDF}^{k,j}(\theta_i, \phi_i; \theta_r, \phi_r; \lambda) = \frac{L_r^{k,j}(\theta_i, \phi_i; \theta_r, \phi_r; \lambda)}{E_i^k(\theta_i, \phi_i; \lambda)} = \frac{P_r^{k,j}(\theta_i, \phi_i; \theta_r, \phi_r; \lambda)}{P_i^k(\theta_i, \phi_i; \lambda)\cos(\theta_r)\Delta\Omega_r} \tag{11}$$

We apply geometric and angular corrections by calculating the instrument function (IF). It is the ratio of the theoretical Lambertian BRDF to a measured Lambertian material BRDF for each angle of incidence

$$\mathrm{IF} = \frac{\mathrm{BRDF}_{\mathrm{Lambertian,\ th}}(\theta_i, \phi_i; \theta_r, \phi_r; \lambda)}{\mathrm{BRDF}_{\mathrm{Lambertian,\ exp}}(\theta_i, \phi_i; \theta_r, \phi_r; \lambda)} = \frac{\mathrm{DHR}(\theta_i, \phi_i; \lambda)/\pi}{\mathrm{BRDF}_{\mathrm{Lambertian,\ exp}}(\theta_i, \phi_i; \theta_r, \phi_r; \lambda)} \tag{12}$$

Figure 6 shows the theoretical and measured in-plane BRDF at 0° lighting at 532 nm of a typical Lambertian material. Spectralon® SRS-99 provided by LabSphere (DHR = 0.99) is used to evaluate the instrument function. IF is close to unity for angles ranging from 0° to 85°: the isotropy and uniformity are verified and corrections are significant only for large angles.

We used three different reference Lambertian samples with different DHR (0.99, 0.70 and 0.50) to process a radiometric calibration. We measured multispectral in-plane BRDF of these samples at 0° light incidence. In these conditions, the in-plane BRDF can be extended to the out-of-plane BRDF to compute the sample's DHR. Moreover, we compared the computed DHR to DHR measurement results from a spectrophotometer (Perkin Elmer Lambda-950 UV/vis/NIR). These results are presented in Tab. 2. The average error found is less than 3% and no additional radiometric calibration is needed for our instrument.

The selection of the incident and detection polarization states is fully automated and calibrated. A polarization analyzer (Meadowlark Optics D3000) is used to characterize polarizers and to align their fast axis. Fresnel equations are also

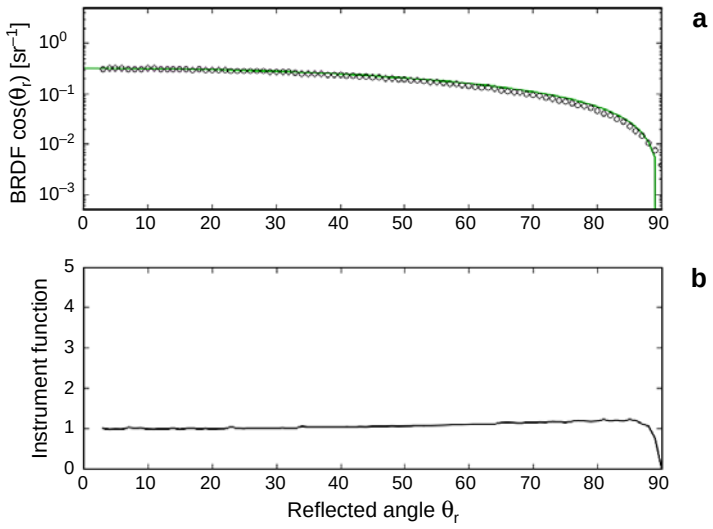

Fig. 6. Geometric calibration results: Spectralon® BRDF (dotted curve) and theoretical Lambertian BRDF (continuous curve) at 0° lightning at 532 nm (**a**) and the associated instrument function (**b**).

T a b l e 2. Radiometric calibration results.

		DHR (LabSphere data)	DHR (spectrophotometer data)	DHR (computed from in-plane BRDF data)
Wavelengths	532 nm	0.990	0.980	0.989
		0.660	0.640	0.653
		0.500	0.506	0.518
	633 nm	0.990	0.989	0.989
		0.650	0.630	0.645
		0.500	0.505	0.520
	814 nm	0.990	0.989	0.989
		0.620	0.610	0.614
		0.500	0.505	0.519

determined from polarized reflection coefficients measured on a germanium wafer with an error less than 2% [18].

Electromagnetic theorems and radiometric analysis are commonly used to demonstrate the BRDF reciprocal property. In other words, if the laser source and the detector are switched, the field amplitude and power are equal. This fundamental property [20] is still available for multiple scattering. For a set of different angles of incidence from 0° to 60°, we verified the reciprocal relation for Lambertian samples with an average error lower than 1%.

Our instrument is fully calibrated for polarized and multispectral in-plane BRDF measurements. In the next section, experimental results are presented and analyzed for various paint coatings (from diffuse to directional coatings).

5. Application to paint coatings

As explained above, light scattering of materials is physically described as the result of surface and subsurface scattering and their BRDFs are decomposed into directional and diffuse components [8]. This decomposition is commonly used although the ratio between the two terms is often arbitrary [18]. We propose to analyze the scattering phenomena for the directional and the diffuse parts of the BRDF with our multispectral polarized-measurements.

5.1. Polarized measurements

From a physical viewpoint, one can explain DOLP values from single or multiple scattering within the media. On the one hand, single scattering or mirror-like reflections do not change the incident polarization state: DOLP is very close to 1. On the other hand, multiple scattering processes do change the polarization state of light: DOLP decreases and is lower than 1.

From experimental results, the BRDF is often separated into two components: directional and diffuse. Table 1 shows the directional component to be mainly due to surface directional scattering and to subsurface directional scattering. It also shows that the diffuse component corresponds to subsurface diffuse scattering and surface diffuse scattering. It is assumed from physical considerations [8] that the polarization state mainly remains almost unchanged for the directional component and is changed for the diffuse component.

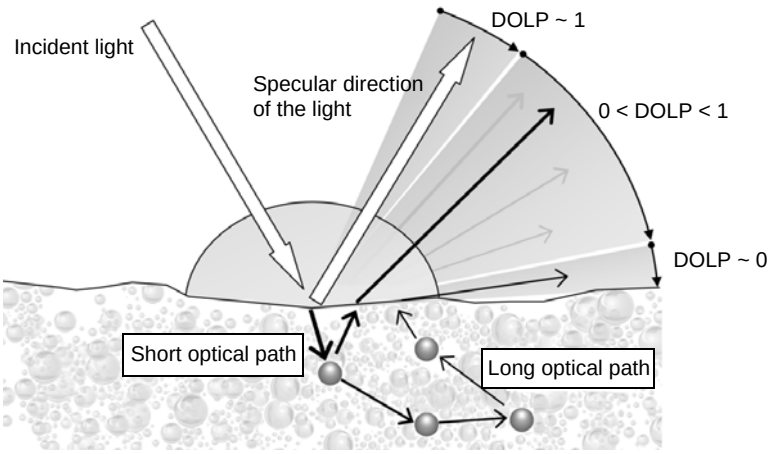

Fig. 7. Angular evolution of the DOLP linked to the light path within the material.

Therefore, the maximum value of the DOLP is always measured at the reflection angle and a lower DOLP is measured apart from the directional component. Also, the DOLP tends to 0 for large angles (Fig. 7) where multiple scattering is dominant for large optical thickness (*i.e.*, long optical path within the material).

Let us study more complex scattering media. The ratio between the different scattering parts impacts directly the BRDF components: the shape of the BRDF is the result of different scattering ratios. Measurements at 532 nm are presented in Fig. 8 for various black paint coatings on aluminium plates with different aspects (matte, matte-glossy and glossy). It shows BRDF and DOLP of these samples: the glossier the paint coating, the more directional the BRDF and the higher the DOLP at reflection angle. From matte to glossy, surface directional scattering contribution is increased compared to subsurface directional scattering: it is measured by higher DOLP values for glossy coatings (Fig. 8).

Polarized measurements are used to separate the different scattering processes in BRDF directional components. DOLP is a useful tool to quantify the ratio between these processes. It tends to 1 when surface directional scattering is high and tends to 0 otherwise (Fig. 8). In order to separate the diffuse components, multispectral measurements should be considered.

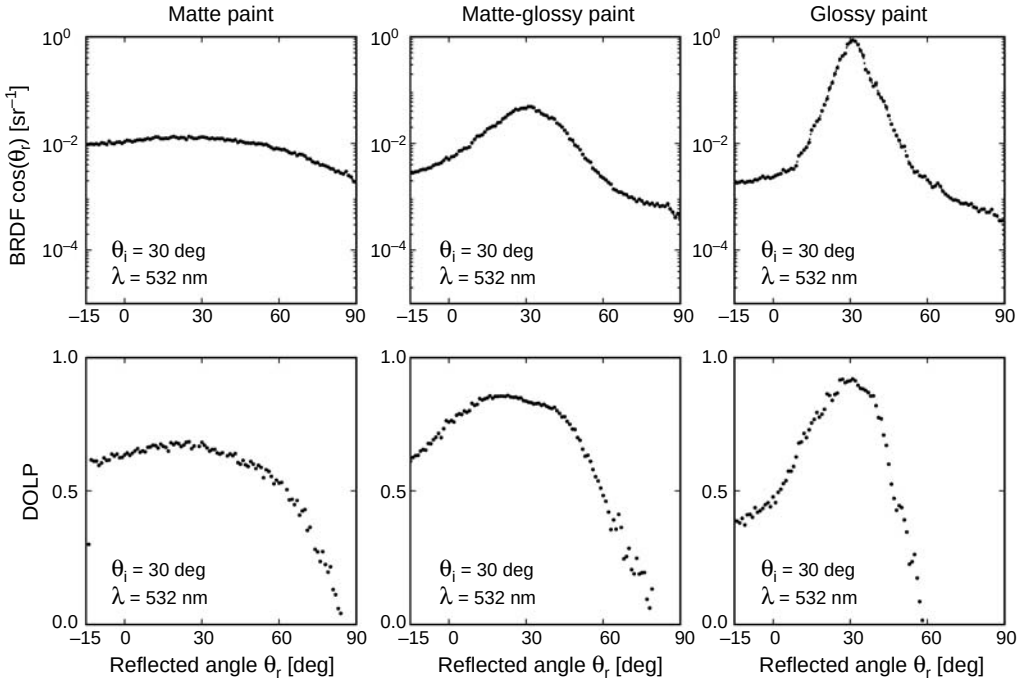

Fig. 8. BRDF (upper figures) and DOLP (lower figures) of a black matte paint coating (left), a black matte-glossy paint coating (center) and a black glossy paint coating (right) at a 30° angle of incidence at 532 nm.

5.2. Multispectral measurements

Multispectral BRDF and DHR of a red glossy paint coating on a polished aluminium plate are measured. Table 3 shows multispectral DHR measurements of the sample at three different wavelengths.

T a b l e 3. Experimental DHR of a red paint coating on an aluminium plate.

Wavelengths	532 nm	633 nm	814 nm
DHR (spectrophotometer data)	0.01	0.47	0.48

Multispectral DHR measurements are carried out to quantify the absorption phenomena in the subsurface: $DHR_{532\ nm} \ll DHR_{633\ nm}$ and $DHR_{532\ nm} \ll DHR_{814\ nm}$. Among the three measured wavelengths, $DHR_{532\ nm}$ is the lowest DHR resulting from a strong absorption phenomena at 532 nm.

In addition, multispectral BRDF measurements are carried out on the same sample to investigate the different scattering phenomena. Figure 9 shows the measured and fitted BRDFs from the Li–Torrance model at the same wavelengths.

Subsurface scattering within the material is spectrally dependent due to different scattering patterns as well as to pigment absorption (related to the relative imaginary refractive index κ) within the media. Therefore, one can use this spectral dependence to distinguish the contribution of the subsurface scattering to the BRDF components.

The directional component of the BRDF is also composed of two scattering terms. One of them is weakly spectral dependent since only a small part of it results from subsurface directional scattering.

Multispectral measurements are used to distinguish the subsurface contribution in the diffuse components of the BRDF.

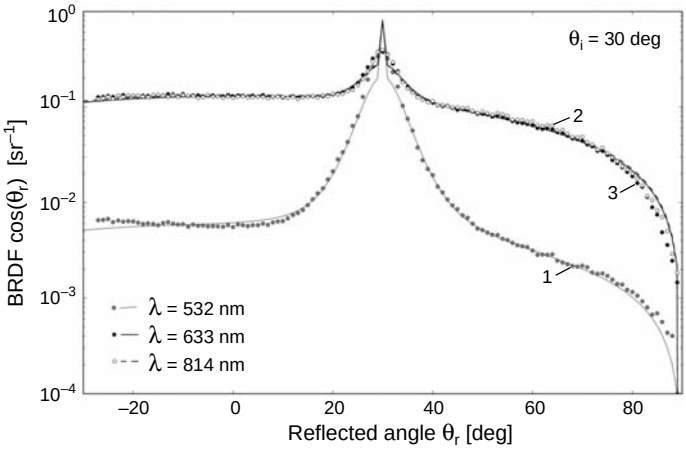

Fig. 9. Measured BRDF (dotted curves) and Li–Torrance BRDF models (solid line) of a red glossy paint coating at a 30° light incidence at 532 nm (grey dotted curve 1), 814 nm (white dotted curve 2) and 633 nm (black dotted curve 3).

5.3. Measurements inversion

In this section, we bring into play our inversion method of measurements. Experimental in-plane multispectral BRDFs of the red paint coating are introduced into our inversion method to retrieve the full BRDF. For this typical red paint coating, we rewrite Eq. (8) for $N = 3$ as:

$$K_N = \begin{bmatrix} k_{dd}^{532} & k_{dd}^{633} & k_{dd}^{814} \\ k_{uds}^{532} & k_{uds}^{633} & k_{uds}^{814} \\ k_{udf}^{532} & k_{udf}^{633} & k_{udf}^{814} \\ k_{fs}^{532} & k_{fs}^{633} & k_{fs}^{814} \end{bmatrix} \tag{13}$$

The multispectral in-plane and full BRDFs computed from this retrieved K_N matrix are presented in Figs. 9–11.

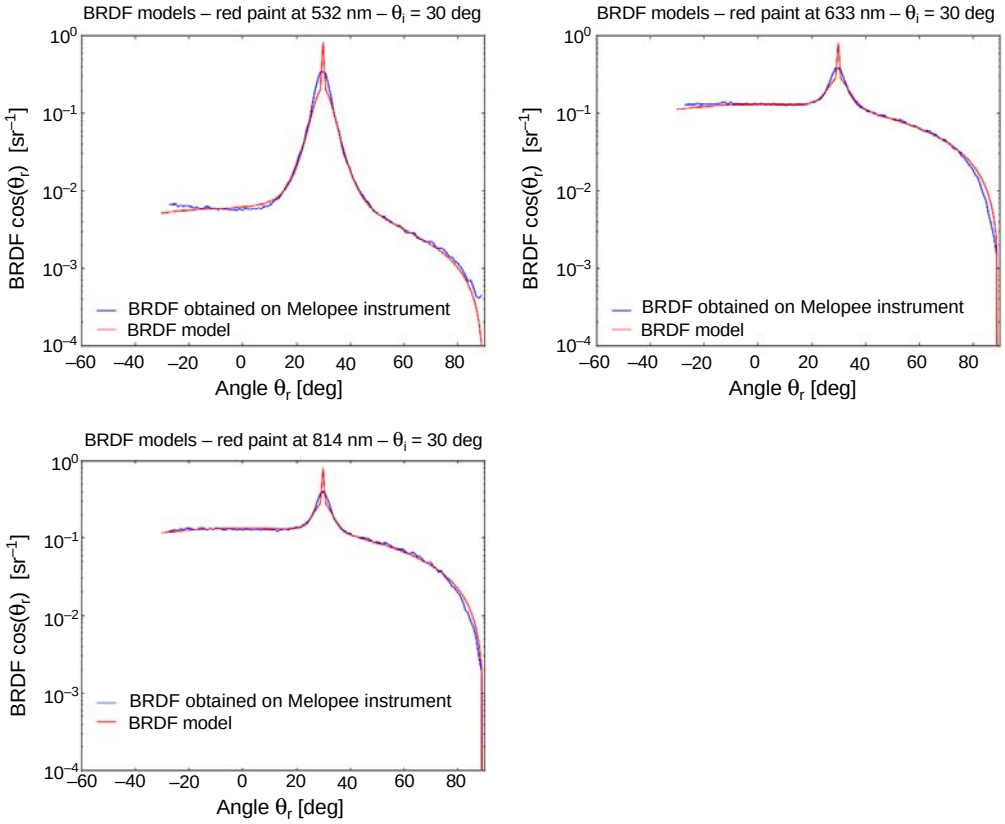

Fig. 10. Multispectral in-plane BRDF of a red paint coating on an aluminium plate (experimental data in blue and model BRDF in red).

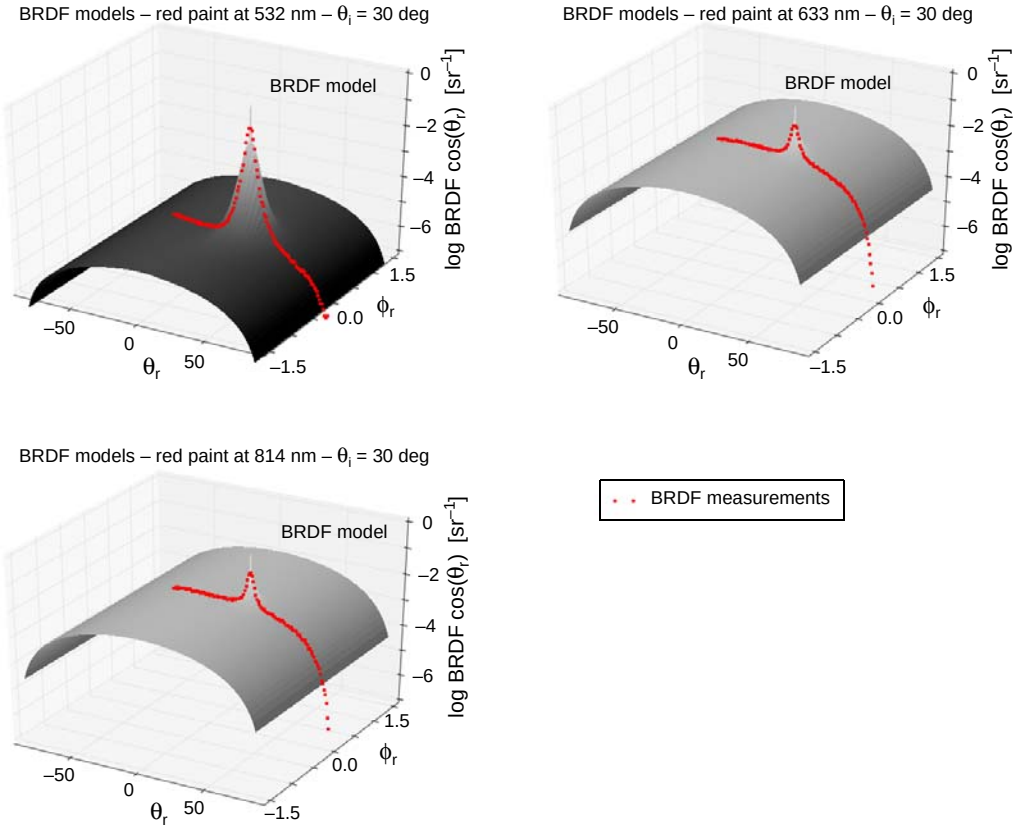

Fig. 11. Multispectral full BRDF of a red paint coating on an aluminium plate (experimental data in red and model BRDF in grey).

As discussed in the previous sections, the diffuse BRDF component is strongly spectral dependent. It is governed by subsurface diffuse scattering which is very spectral dependent. Thus, BRDF diffuse components are quite lower at 532 nm than those at 633 nm and 814 nm.

To take these physical considerations into account, the Li–Torrance model input parameters (such as n, κ and DHR) were optimized giving additional conditions: $\kappa_{532\ \mathrm{nm}} \gg \kappa_{633\ \mathrm{nm}}$ or $\kappa_{814\ \mathrm{nm}}$ and $\mathrm{DHR}_{532\ \mathrm{nm}} \gg \mathrm{DHR}_{633\ \mathrm{nm}}$ or $\mathrm{DHR}_{814\ \mathrm{nm}}$. The resulting k-parameters are presented in Tab. 4.

T a b l e 4. Experimental DHR and Li–Torrance DHR of a red paint coating on an aluminium plate.

Wavelengths	532 nm	633 nm	814 nm
Li–Torrance k_{udf}	0.0162	0.0300	0.0001
Li–Torrance k_{uds}	0.0028	0.4860	0.4914
DHR (inversion method)	0.0190	0.4890	0.4915

From our inversion method, the modelled multispectral full BRDF and the multispectral DHR were retrieved with an error lower than 1%.

6. Conclusions

An instrument for studying the light scattered by materials has been designed at Onera. Our instrument measures in-plane multispectral polarized-BRDF and DOLP with a high angular resolution. Such measurements can be either used for a physical analysis of the optical surface signature or for applications such as laser-imaging simulation codes using the full BRDF.

Based on our measurements on paint coatings, we discussed how to dissociate surface and subsurface scattering processes in the BRDF components. Polarized and multispectral measurements quantify the different scattering ratios from directional and diffuse BRDF components, respectively. This method was applied to various paint coatings to illustrate the potential of the method as a surface quality control tool.

We also introduced a data inversion technique. The full BRDF and multispectral DHR are retrieved from multispectral in-plane measurements for different angles of incidence and for either diffuse or specular media.

References

[1] Myoung Kook Seo, Kang Yeon Kim, Duck Bong Kim, Kwan H. Lee, *Efficient representation of bidirectional reflectance distribution functions for metallic paints considering manufacturing parameters*, Optical Engineering **50**(1), 2011, article 013603.

[2] Voss K.J., Chapin A., Monti M., Zhang H., *Instrument to measure the bidirectional reflectance distribution function of surfaces*, Applied Optics **39**(33), 2000, pp. 6197–6206.

[3] Brakke T.W., *Goniometric measurements of light scattered in the principal plane from leaves*, Proceedings of Geoscience and Remote Sensing Symposium, IGARSS, 1992.

[4] Jafolla J.C., Thomas D.J., Hilgers J.W., Reynolds W.R., Blasband C., *Theory and measurement of bidirectional reflectance for signature analysis*, Proceedings of SPIE **3699**, 1999, p. 2.

[5] Leloup F.B., Forment S., Dutre P., Pointer M.R., Hanselaer P., *Design of an instrument for measuring the spectral bidirectional scatter distribution function*, Applied Optics **47**(29), 2008, pp. 5454–5467.

[6] Chunnilall C.J., Clarke F.J.J., Smart M.P., Hanssen L.M., Kaplan S.G., *NIST–NPL comparison of mid-infrared regular transmittance and reflectance*, Metrologia **40**(1), 2003, pp. 55–59.

[7] Betty C.L., Fung A.K., Irons J., *The measured polarized bidirectional reflectance distribution function of a Spectralon calibration target*, Proceeding of Geoscience and Remote Sensing Symposium, Vol. 4, 1996, pp. 2183–2185.

[8] Ellis K.K., *Polarimetric bidirectional reflectance distribution function of glossy coatings*, Journal of the Optical Society of America A **13**(8), 1996, pp. 1758–1762.

[9] Haner D.A., McGuckin B.T., Bruegge C.J., *Polarization characteristics of Spectralon illuminated by coherent light*, Applied Optics **38**(30), 1999, pp. 6350–6356.

[10] Nicodemus F.E., *Directional reflectance and emissivity of an opaque surface*, Applied Optics **4**(7), 1965, pp. 767–773.

[11] Haner D.A., McGuckin B.T., Menzies R.T., Bruegge C.J., Duval V., *Directional-hemispherical reflectance for Spectralon by integration of its bidirectional reflectance*, Applied Optics **37**(18), 1998, pp. 3996–3999.

[12] BECKMANN P., *Shadowing of random rough surfaces*, IEEE Transactions on Antennas and Propagation **13**(3), 1965, pp. 384–388.
[13] XIAO D. HE, TORRANCE K.E., SILLION F.X., GREENBERG D.P., *A comprehensive physical model for light reflection*, ACM SIGGRAPH Computer Graphics **25**(4), 1991, pp. 175–186.
[14] TORRANCE K.E., SPARROW E.M., *Theory for off-specular reflection from roughened surfaces*, Journal of the Optical Society of America **57**(9), 1967, pp. 1105–1112.
[15] COOK R.L., TORRANCE K.E., *A reflectance model for computer graphics*, ACM Transactions on Graphics (TOG) **1**(1), 1982, pp. 7–84.
[16] LI H., TORRANCE K.E., *A practical, comprehensive light reflection model*, Program of Computer Graphics, Technical Report PCG-05-03, Cornell University, 2005.
[17] PHONG B.T., *Illumination for computer generated images*, Communications of ACM **18**(6), 1975, pp. 311–317.
[18] NOCEDAL J., WRIGHT S.J., *Numerical Optimization*, 2nd Ed., Springer-Verlag, Berlin, New York, 2006.
[19] LI H., TORRANCE K.E., *Validation of the Gonioreflectometer*, Program of Computer Graphics, Technical Report PCG-03-02, Cornell University, 2003.
[20] SEARS F.W., *Optics*, Addison-Wesley Press, 1949.

Received May 16, 2011
in revised form August 31, 2011